Response linearity in primary auditory cortex of the ferret

Bashir Ahmed, Jose A. Garcia-Lazaro and Jan W. H. Schnupp

Department of Physiology, Anatomy and Genetics, University of Oxford, Sherrington Building, Parks Road, Oxford OX1 3PT, UK

The responses of neurons within the primary auditory cortex (A1) of the ferret elicited by broadband dynamic spectral ripple stimuli were examined over a range of ripple spectral densities and ripple velocities. The large majority of neurons showed modulated responses to these stimuli and responded most strongly at low ripple densities and velocities. The period histograms of their responses were subjected to Fourier analysis, and the ratio of the magnitudes of the f_1 and f_0 (DC) components of these responses were calculated to give a quantitative index of response linearity. For 82 out of 396 neurons tested (20.7%) this ratio remained above 1.0 over the entire range of ripple densities and velocities. These neurons were classified as 'consistently linear'. A further 134/396 (33.8%) of neurons maintained an f_1/f_0 ratio above 1.0 for either a range of ripple densities at a fixed ripple velocity, or over a range of ripple velocities at a specific ripple density, and were classified as 'locally linear'. Interestingly, for the superficial layers of the primary auditory cortex, consistently linear and locally linear neurons outnumbered nonlinear neurons by a 2:1 ratio. The converse was true for the deep layers. Unlike in primary visual cortex, where f_1/f_0 ratios have been reported to exhibit a bimodal distribution with a minimum at $f_1/f_0 \approx 1$, f_1/f_0 ratios for A1 are unimodally distributed with a peak at $f_1/f_0 \approx 1$.

(Resubmitted 23 December 2005; accepted after revision 19 February 2006; first published online 23 February 2006)
Corresponding author B. Ahmed: Department of Physiology, Anatomy and Genetics, University of Oxford, Sherrington Building, Parks Road, Oxford OX1 3PT, UK. Email: bashir.ahmed@physiol.ox.ac.uk

Previous studies have revealed a tonotopic organization within the primary auditory cortex (A1) (Merzenich *et al.* 1973), as well as a clustering of basic functional properties within isofrequency contours (Schreiner & Mendelson, 1990; Nelken, 2002; Read *et al.* 2002), but so far no specific, fundamental, feature selectivity has been found which might underlie its functional organization, and which can be systematically mapped across its surface or perpendicularly through its depth. Clearly, individual neurons do show spectral tuning to frequency and intensity (Merzenich *et al.* 1975; Phillips & Irvine, 1981). They show selectivity to sounds modulated in amplitude (Schreiner & Urbas, 1988) and frequency (Mendelson & Cynader, 1985; Nelken & Versnel, 2000), but to rates of a few tens of cycles per second (Lu *et al.* 2001; Joris *et al.* 2004). In order to predict feature selectivities of auditory cortical neurons, a number of studies have used correlational analysis between the spectrotemporal structure of the sound and the neuronal response (Aertsen & Johannesma, 1981; deCharms *et al.* 1998; Sen *et al.* 2001; Schnupp *et al.* 2001). These approaches have estimated a neuron's 'spectrotemporal receptive field', with acoustic stimuli ranging from broadband sounds with sinusoidal modulation of both frequency and amplitude (Kowalski *et al.* 1996*a*,*b*), random chord sequences (deCharms *et al.* 1998; Schnupp *et al.* 2001; Rutkowski *et al.* 2002), and natural stimuli, including animal vocalizations (Theunissen *et al.* 2000; Sen *et al.* 2001). The underlying assumption in these studies has been response linearity based on stimulus–response stationarity, i.e. the effect of the preceding stimulus is assumed to be negligible on the response to the next stimulus. These approaches provide indirect and qualitative estimates of neuronal linearity. Clearly, there is a requirement for an approach that can gauge the degree of linearity. This would provide a quantitative measure of linearity for auditory cortical neurons. We have employed an approach analogous to a method commonly used in studies of primary visual cortex (V1) to generate quantitative estimates of response linearity for neurons in the primary auditory cortex of ferrets.

The landmark studies of Hubel & Wiesel (1959, 1962, 1968) on the primary visual cortex led them to distinguish two major neuron classes which they termed 'simple' and 'complex'. Based on a series of qualitative measures of spatial summation, they were able to show that simple-type cells were approximately linear in their responses compared with the non-linear complex cells. An approach to assess linearity of spatial summation of visual cortical neurons quantitatively was first described by Movshon *et al.* (1978*a*,*b*) with a grating where the luminance was sinusoidally modulated (sine-wave grating). The

 DOI: 10.1113/jphysiol.2005.104380

equivalent of a sine-wave grating in the auditory domain is the dynamic spectral ripple stimulus (Shamma *et al.* 1995; Shamma & Versnel, 1995; Versnel *et al.* 1995; Kowalski *et al.* 1996*a*,*b*). Ripple stimuli are broad-band sounds that exhibit time-varying spectral modulation. In practice, these stimuli are synthesized from a large number (>100) of individually amplitude modulated pure-tone components which are equally spaced along the logarithm of the frequency axis (0.5–25 kHz). The Fourier transform of this dynamic spectral ripple stimulus has a single component within the domains of ripple frequency and ripple velocity (and its complex conjugate). Consequently, it is possible to undertake with this stimulus on auditory neurons the equivalent type of analysis that Movshon *et al.* (1978*a*,*b*,*c*) undertook on V1 neurons and, hence, obtain a quantitative estimate of the neuron's response linearity *known as the* f_1/f_0 *ratio*. In V1, f_1/f_0 ratios are bimodally distributed: linear 'simple' cells tend to have f_1/f_0 ratios greater than one, while non-linear, 'complex' cells have f_1/f_0 ratios less than one, and only relatively few neurons have f_1/f_0 values very close to one. The f_1/f_0 ratio therefore provides a convenient and natural criterion for distinguishing physiological response classes in V1. Interestingly, if visual afferents are surgically re-routed to terminate in A1 rather than V1 in a developmentally very immature animal, then 'simple' and 'complex' visual response classes can emerge in A1 that has been targeted by visual inputs (Roe *et al.* 1992). It is therefore pertinent to ask whether 'simple' and 'complex' response classes might be a 'natural' feature of sensory cortices, which might also be observed among auditory responses of normal A1 if these are analysed using the acoustic equivalent of the sinusoidally modulated luminance grating stimuli commonly used to quantitatively discriminate simple from complex cells in V1.

In this paper we describe the distribution of f_1/f_0 ratios that were obtained with dynamic spectral ripple stimuli from the primary auditory cortex of the anaesthetized adult ferret. In ferret auditory cortex we found approximately half of all neurons driven by the ripple stimuli to have f_1/f_0 ratios greater than one, but f_1/f_0 ratios compiled over the entire population of A1 neurons were unimodally distributed with a mode near one. Furthermore, we found high f_1/f_0 ratios which would be indicative of linear neurons to be more commonly found in the superficial layers of A1.

Methods

Animal preparation

Two adult pigmented female ferrets (*Mustela putorious*) were used in this study. Otoscopic examinations were performed a few days in advance and on the day of the experiment to ensure that both ears were clean and disease free.

Anaesthesia was induced by 2.0 ml kg^{-1} intramuscular injection of alphaxalone/alphadolone acetate (Saffan; Schering-Plough Animal Health, Welwyn Garden City, UK) and maintained, during the surgery, by intravenous injection of supplementary doses when required. Once surgery was complete, anaesthesia was maintained by continuous I.V. infusion through the left radial vein of a mixture of medetomidine (Domitor; Pfizer) and ketamine (Ketaset; Fort Dodge Laboratories) at, respectively, 0.022 and 5 mg kg^{-1} h^{-1} in saline (2 ml h^{-1}). In addition, a continuous infusion (5 ml h^{-1}) of saline supplemented by glucose 5%, dexamethasone (Dexadreson) 0.5 mg kg^{-1} h^{-1}, and atropine sulphate 0.06 mg kg^{-1} h^{-1}, was maintained throughout the experiment. A tracheal cannula was inserted for artificial ventilation and an oxygen-rich, air mixture was administered to maintain end-tidal CO_2 at approximately 3.8%.

The animal was placed in a stereotaxic frame and the temporal muscles of both sides were retracted to expose the dorsal and lateral parts of the skull. Along the midline of the skull a metal bar was screwed in place and cemented with dental acrylic to hold the head without the need of a stereotaxic frame. On the left side, the temporal muscle was retracted and a craniotomy was performed overlying the primary auditory cortex. The overlying dura was removed and the exposed area was filled with silicon oil. A speculum was inserted into each ear canal and aligned autoscopically. For acoustic stimulation, earphones (Panasonic RPHV297, Bracknell, UK) were inserted and held in place within each of the specula. Body temperature, expired CO_2, electrocardiogram (ECG) and heart rate measurements were carefully monitored to ensure stable and adequate anaesthesia. Adequacy of anaesthetic depth was established by the absence of flexor withdrawal reflex and by an assessment of muscle tone during application of painful pressure to front or hind paws. We undertook this assessment intermittently throughout the duration of the experiment, and without delay if there were any significant changes in breathing or heart rate. All procedures were performed under licence from the UK Home Office in accordance with the Animal (Scientific Procedures) Act 1986. At the end of the recording experiments, the animals were overdosed with intravenous pentobarbitone (Euthatal, Merial).

Stimulation and recording

The stimuli were broadband dynamic ripple spectra (0.5–25 kHz, duration 30 s, 3–5 repeats, randomly interleaved, presented diotically), varying in density (0.125–2 cycles oct^{-1}) and velocity (0.5–16 Hz). The range

of densities and velocities varied somewhat across different recording locations, the usual range was 0.25–2.0 cycles oct^{-1} in density and 1–8 Hz in velocity. In addition, pure tones of duration 100 ms (rise and fall times of 5 ms, every 750 ms) were presented to the contralateral ear over a frequency range of 0.5–25 kHz and sound intensities of 10–70 dB SPL. All stimuli were generated through a TDT System3 real-time signal processor (RP 2.1; Tucker Davis Technologies, Alachua, FL, USA).

Extracellular recordings were performed in a purpose-built, sound-proof, anechoic sound-attenuated chamber (Industrial Acoustics Company Ltd, Winchester, UK), using 2.5 MΩ silicon array electrodes (16 recording sites, arranged as four sites on four shanks or as 16 sites on a single shank at a 100 μm separation. University of Michigan, Centre for Neural Communication Technology, MI, USA).

The signals were bandpass filtered (300–3 kHz), amplified (up to 30 000), and digitized at 25 kHz with a TDT RX5 64-channel Pentusa BioAmp recording system. The BrainWare software (TDT; Gainseville, FL, USA) was used to control stimulus presentation and data collection. Single and multiunit activity was isolated from the digitized signal by setting a threshold level above the mean noise level and these spike waveforms (duration, 1 or 2 ms) were then recorded onto the hard disc for offline cluster cutting and analysis.

Data analysis

The acquired spike waveforms were separated into single units by examining a range of parameters of the recorded spike waveforms with the analysis tools available in BrainWare (TDT). These are based on a dual-axis

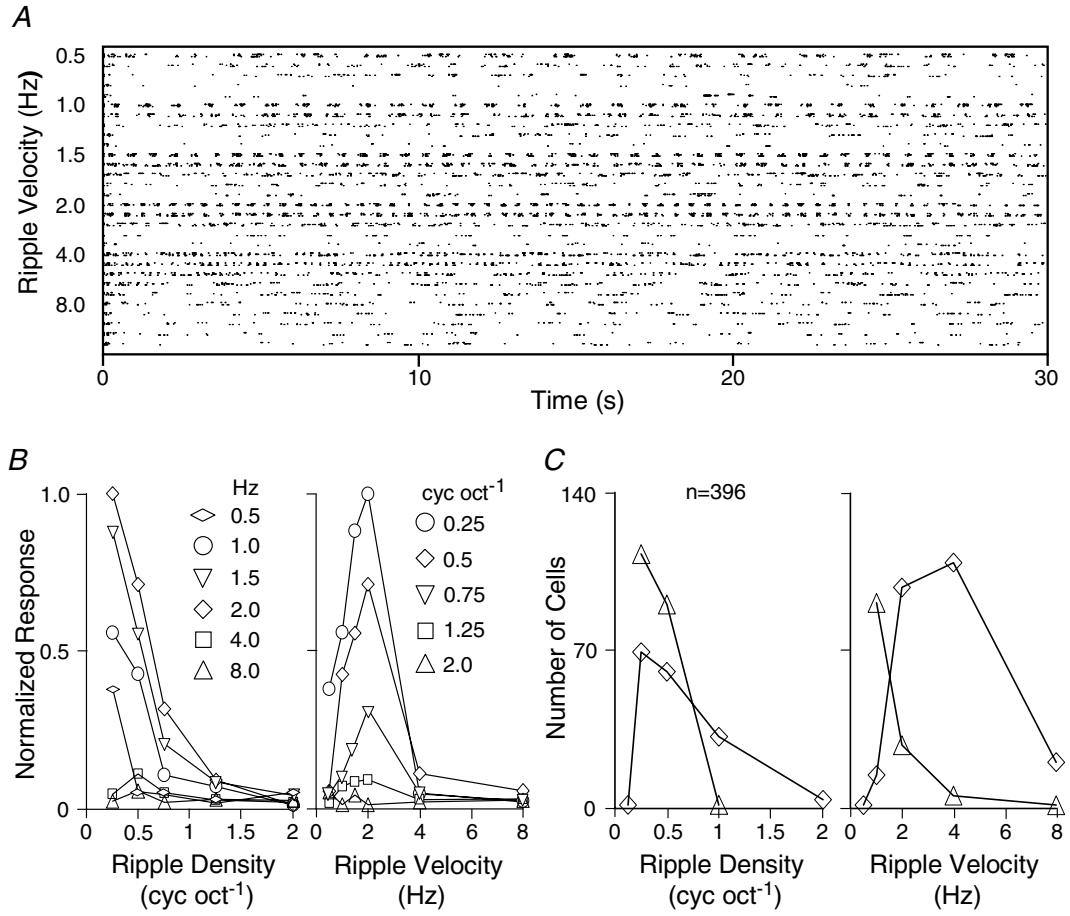

Figure 1. Tuning characteristics of neurons to dynamic spectral ripple stimuli
A, raster plot (duration, 30 s) of the response of a neuron to a range of ripple velocities (0.5–8 Hz) and ripple densities (0.25–2 cycles oct^{-1}) at each velocity. *B*, the tuning characteristics of this neuron. Responses (normalized) are plotted to a range of ripple densities (left) and a range of ripple velocities (right). This neuron's peak response was elicited at a ripple velocity of 2 Hz and a ripple density of 0.25 cycles oct^{-1}. *C*, summary of the tuning characteristics of our population of neurons ($n = 396$). ◇, distribution of neurons tuned to a particular density (left) or velocity (right). △, neurons that preferred a particular density (left) or velocity (right) but were not clearly tuned.

clustering of parameters derived from spike waveforms (e.g. spike amplitude, time to trigger, area of spike waveform, duration between crossing of trigger levels by spike waveform, etc.), followed by autocorrelational analysis of spike timing as a test of individual spike clusters. Single clusters, so defined, were assumed to represent single units, and their spike responses to the auditory stimuli were analysed. For a given spectral ripple stimulus (for example, at a fixed density of 0.25 cycles oct^{-1} and a velocity of 2 Hz), an averaged period histogram (295 stimulus cycles determined over a duration from the second stimulus cycle to 30 s) was constructed from the 3–5 random stimulus presentations. The first stimulus cycle of each presentation was excluded from this analysis to prevent any stimulus-onset nonlinearity in the neuronal response. Discrete Fourier analysis (Matlab; The Mathworks, Inc., Natick, MA, USA) of this period histogram, after subtracting the ongoing spontaneous spike activity, gave the magnitudes of the response components at the zero frequency (the unmodulated DC component, f_0), and at the stimulus frequency (the modulated component, f_1). We computed the f_1/f_0 ratio. This ratio provides a quantitative estimate of linearity (Movshon *et al.* 1978*a*,*b*). Those and other authors examined responses to a limited range of spatial frequencies of the sinusoidally modulated grating and, in many cases, only to a single spatial frequency which gave the peak response (Movshon *et al.* 1978*a*,*b*; Dean & Tolhurst, 1983; Skottun *et al.* 1991) to characterize the neuron's relative modulation. We have defined linearity more strictly for our sample by classifying neurons as 'consistently linear' only if the relative modulation was maintained above a ratio of

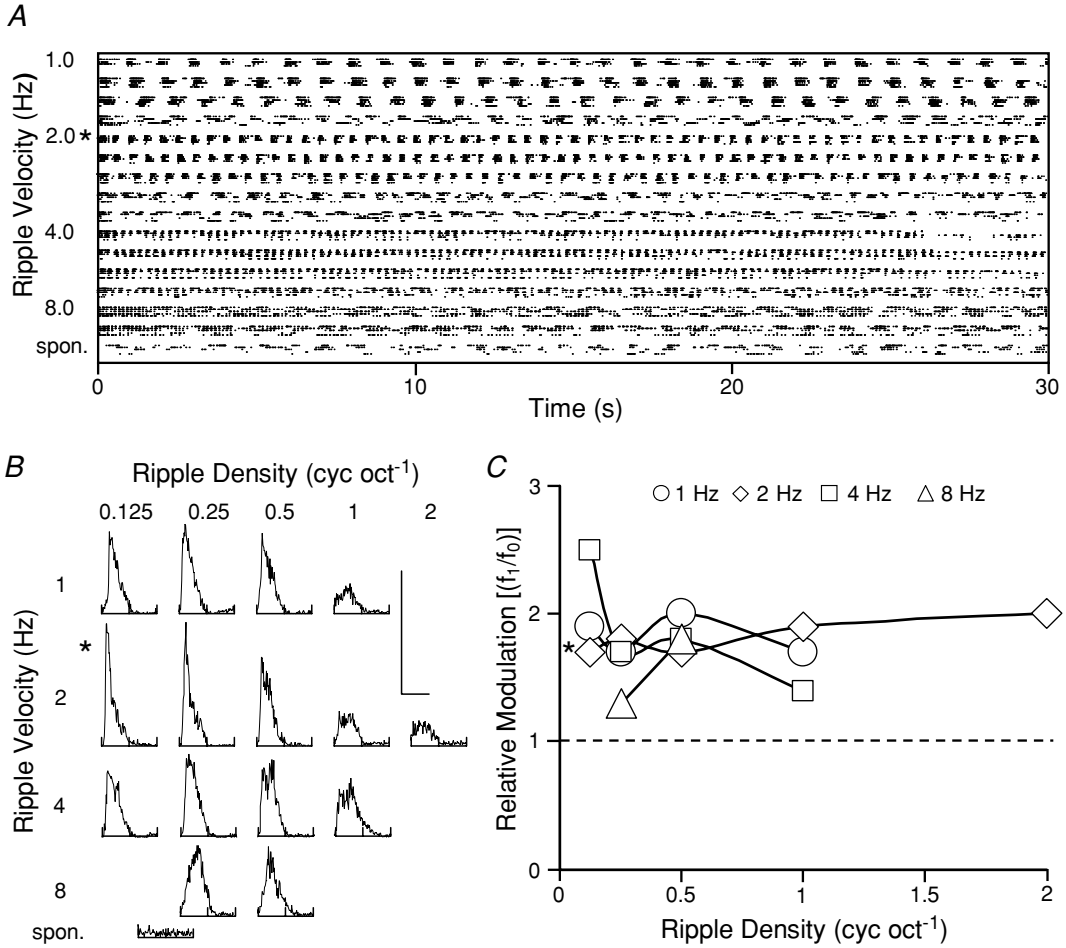

Figure 2. Responses of an A1 neuron classified as consistently linear
A, spike discharge as a raster display for a range of ripple velocities (1–8 Hz) and densities (0.125–2 cycles oct^{-1}), as well as ongoing spontaneous activity. *B*, respective period histograms constructed from the five presentation runs, but over the duration from the second stimulus cycle to 30 s of the ripple presentation. Calibration bars: vertical bar, 150 spikes bin^{-1}; horizontal bar, 500–62.5 ms (1–8 Hz). The period histogram was Fourier transformed, and the discrete components f_1 and f_0 for each period histogram were determined. These are plotted as a ratio (f_1/f_0) in *C* for the range of ripple velocities and densities. This neuron was classified as consistently linear as the f_1/f_0 ratio remained above 1.0 (at best response*, the f_1/f_0 ratio was 1.7, and the mean ± S.D. was 1.79 ± 0.27).

1.0 for the full range of ripple stimuli to which the neuron was responsive. Conversely, we classified neurons with f_1/f_0 ratios consistently below 1.0 across all stimuli as 'consistently non-linear'. Furthermore, we classified neurons as 'locally linear' if this ratio was maintained at or above 1.0 for either a range of ripple densities (from 0.25 to 2 cycles oct^{-1}) for a given ripple velocity (e.g. 2 Hz) or a range of ripple velocities (from 1 to 8 Hz, and occasionally 16 Hz) at a given ripple density (e.g. 0.5 cycles oct^{-1}). A large number of neurons alternated in this ratio between >1.0 or <1.0 over the full range of ripple stimuli. These neurons were classified as 'inconsistent non-linear'.

Results

From a total population of 608 primary auditory cortical neurons, 455 had significant responses to dynamic spectral ripple stimuli. Fifty-nine of these neurons, however, only responded to a single ripple stimulus or a limited range of these ripple stimuli. The remaining population of cortical neurons were well driven over a wide range of ripple stimuli. The tuning characteristics of these 396 neurons were analysed and the majority were found to prefer low ripple densities (<0.5 cycles oct^{-1}) and velocities (<8 Hz). In Fig. 1 we show the distribution of these results. Figure 1*A* shows a raster plot for a neuron. The responses cover a range of ripple densities (0.25–2 cycles oct^{-1}) and ripple velocities (0.5–8 Hz) and were recorded over a duration of 30 s (three presentations, randomly interleaved). On presentation of the ripple sound, the majority of neurons showed responses to the ripple stimulus, and an onset-mediated response to the very first cycle of stimulus presentation. Consequently, the first stimulus cycle of the response was excluded from the data analysis, and the

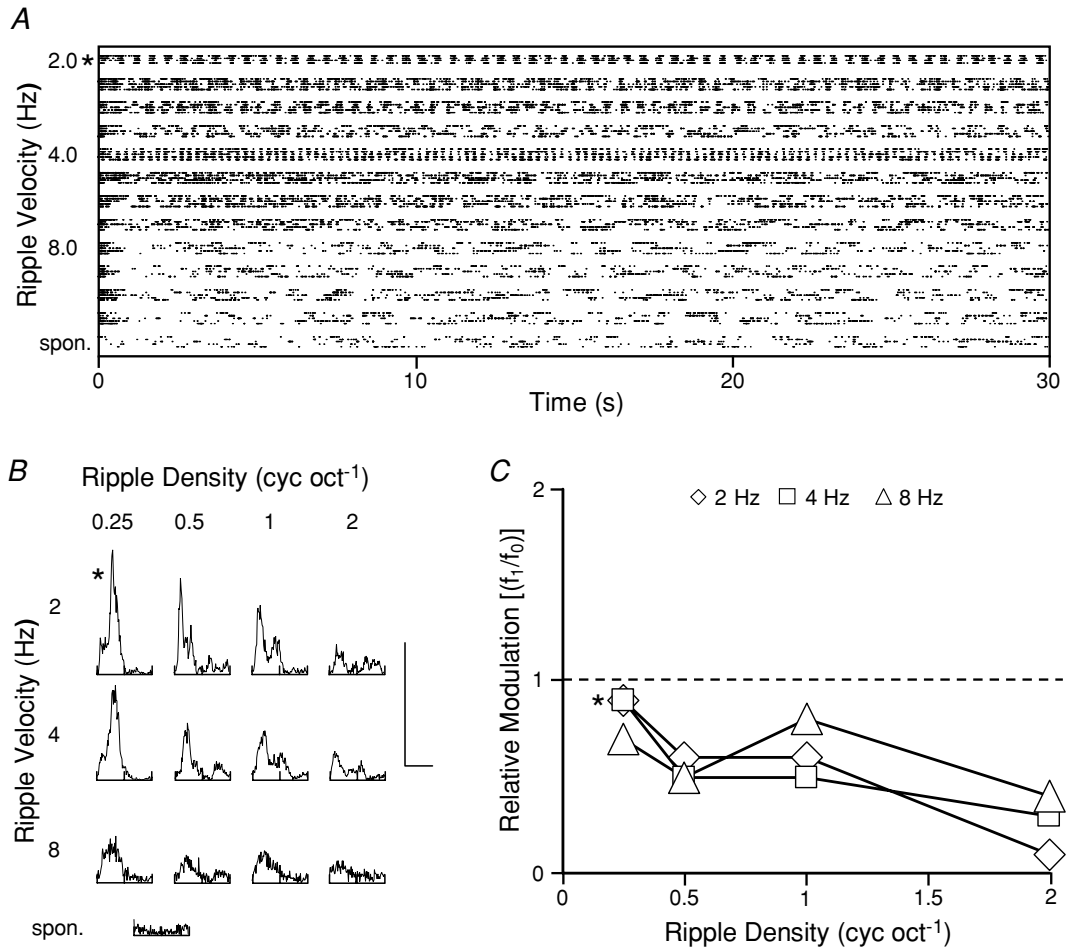

Figure 3. Responses of a consistently nonlinear A1 neuron
A, raster plot, with the neuron's responses as period histograms in *B*, for dynamic ripple stimuli varying in density (0.25–2 cycles oct^{-1}) and frequency (2–8 Hz). Calibration bars: vertical bar, 250 spikes bin^{-1}; horizontal bar, for 250 ms (2 Hz), 125 ms (4 Hz), and 8 Hz, 125 spikes bin^{-1} and 62.5 ms. The f_1/f_0 ratios are plotted in *C*. This ratio remained below 1.0 for this neuron (at best response*, the f_1/f_0 ratio was 0.9, and mean $\pm$ S.D. was 0.57 $\pm$ 0.24) and, accordingly, the neuron was classified as consistently non-linear.

modulated spike activity was analysed from the second stimulus cycle to the last stimulus cycle. The neuron shown in Fig. 1 was tuned to a ripple density of 0.25 cycles oct^{-1} (Fig. 1*B*, left) and a ripple velocity of 2 Hz (Fig. 1*B*, right). In Fig. 1*C* we show the tuning characteristics of our sample population. For ripple density (Fig. 1*C*, left), the peak responses from neurons were elicited at or below 1 Hz (24.9%) or were tuned, with the majority preferring a velocity of 4 Hz (29.7%). Similarly for ripple velocity (Fig. 1*C*, right), peak responses occurred for neurons at or below 0.25 cycles oct^{-1} (30.5%) or were tuned around this density (18.7%). Most neurons (44.3%) therefore gave peak responses at a ripple velocity and density of, respectively, 1 Hz and 0.25 cycles oct^{-1}.

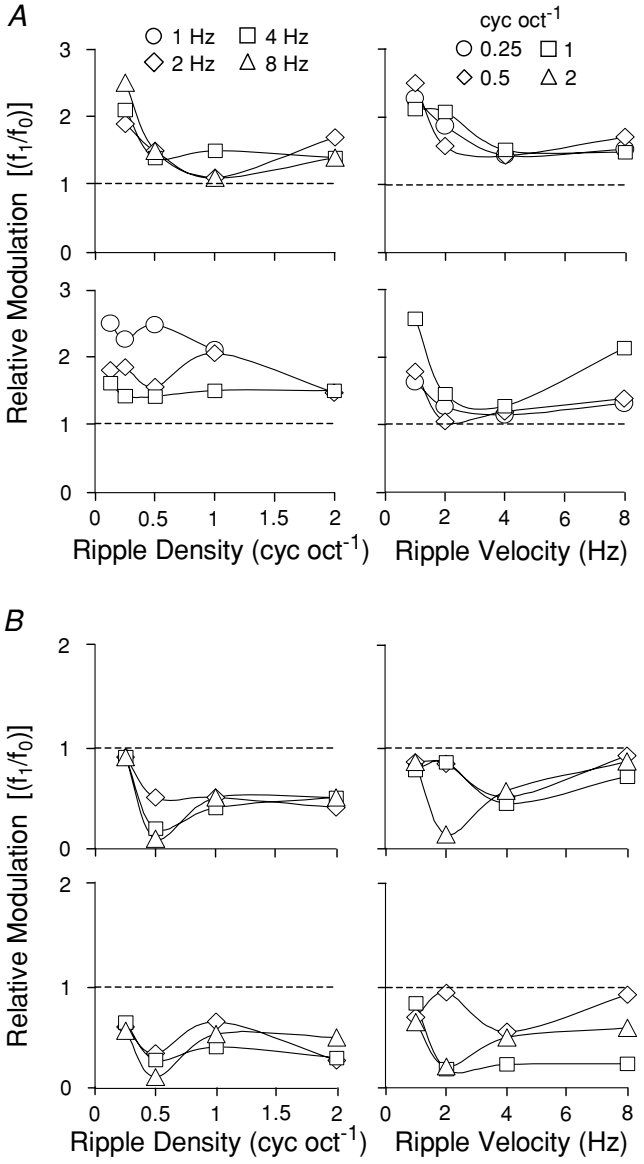

Figure 4. Relative modulation ratios for neurons from A1
A, examples of the ratios for four consistently linear neurons ($f_1/f_0 > 1.0$). The two examples on the left are at fixed ripple densities over the range of ripple velocities, and the examples on the right are at fixed ripple velocities over the range of ripple densities. *B*, equivalent data for neurons classified as consistently non-linear ($f_1/f_0 < 1.0$).

In Fig. 2 we show the complete data set for a neuron which we classified as 'consistently linear'. Figure 2*A* shows the raster plot for this neuron. The responses cover a range of ripple densities (0.125–2 cycles oct^{-1}) and ripple velocities (1–8 Hz; five presentations, randomly interleaved). Period histograms of these responses are shown in Fig. 2*B*, together with the ongoing spontaneous spike activity for this neuron. We examined the responses in each of these period histograms by Fourier analysis to obtain the magnitudes of the f_1 and f_0 components for each ripple velocity and density, and then calculated the f_1/f_0 ratio. These ratios are plotted in Fig. 2*C* for the range of ripple densities at the four ripple velocities of 1, 2, 4 and 8 Hz. For this neuron, the ratios remained above 1.0 and, hence, this neuron was classified as consistently linear (mean ± s.d., 1.79 ± 0.27). The ratio at the best response for this neuron (ripple velocity 2 Hz, ripple density 0.125 cycles oct^{-1}) was 1.7. In Fig. 3, a second example is shown but for a neuron where the f_1/f_0 ratio was always below 1.0. Hence, this neuron was classified as 'consistently nonlinear'. A number of the period histograms (Fig. 3*B*) showed two responses per presentation cycle, i.e. a clear period doubling in the response and, consequently, this is an unambiguous example of a neuron with nonlinear behaviour. Similarly, the f_1/f_0 ratios are plotted in Fig. 3*C* for this neuron. The ratios at the best response (ripple velocity 2 Hz, ripple density 0.25 cyc oct^{-1}) as well as the overall mean (±s.d.) were 0.9 and 0.57 (±0.24), respectively. This neuron therefore processed all dynamic ripple sounds (within our experimental range) nonlinearly. Within our experimental range of ripple stimuli, neurons with ratios greater than 1.0 throughout numbered 82 and were classified as 'consistently linear', while 62 neurons maintained an f_1/f_0 ratio below 1.0 and were classified as 'consistently non-linear'. Typical examples of the range of ratios are shown in Fig. 4 (Fig. 4*A*, consistently linear neurons; Fig. 4*B*, consistently non-linear neurons). These neurons were, however, exceptional, because most of the neurons ($n = 252$) exhibited f_1/f_0 ratios which were sometimes above and sometimes below 1.0. That is there was a dependence of this ratio on the precise ripple velocity and density. A subgroup of these neurons maintained an f_1/f_0 ratio above 1.0 at either a constant ripple velocity over a range of ripple densities (Fig. 5*A*, *Ba* and *Bb*) or at a constant ripple density for a range of ripple velocities (Fig. 5*Bc* and *Bd*). We classified these neurons as 'locally linear' ($n = 134$, 33.8%). The remaining neurons alternated in their f_1/f_0 ratios between above and below 1.0 with no systematic relationship to the densities or velocities of the dynamic

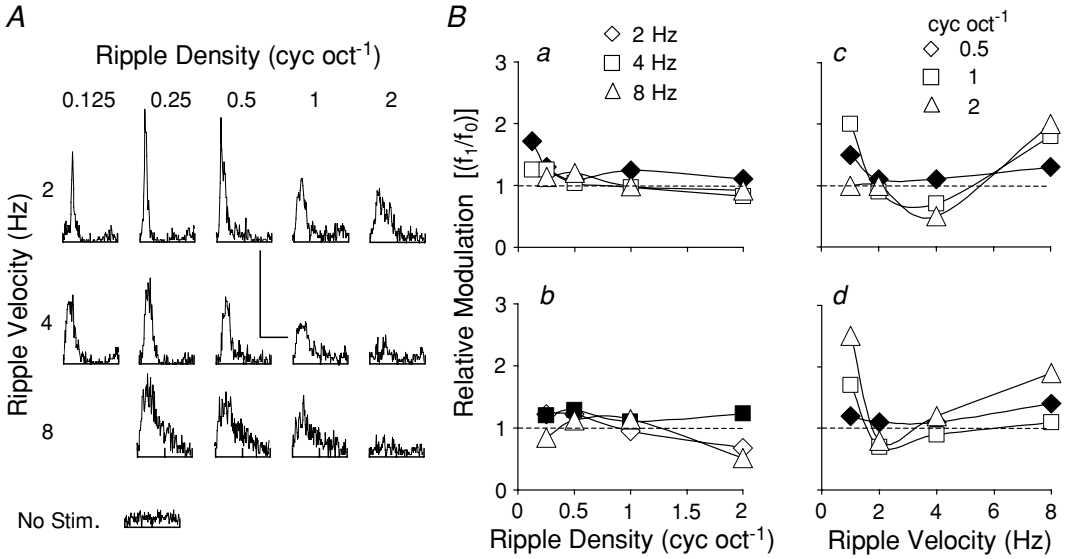

Figure 5. Responses from neurons classified as locally linear
A, period histograms for a neuron over ripple velocities (2, 4 and 8 Hz) and densities (0.125–2 cycles oct^{-1}). The calibration bars represent 60 spikes bin^{-1} and duration of 250 ms at 2 Hz, 60 spikes bin^{-1} and 125 ms at 4 Hz, and 30 spikes bin^{-1} and 62.5 ms at 8 Hz. *Ba*, f_1/f_0 ratios for the data. At 2 Hz ripple velocity the ratios remained above 1.0 (♦) for the range of ripple densities. Similarly, data for three other neurons (*b–d*) are shown. Filled symbols, ratios which remained above 1.0 on a continuous scale of ripple velocity or density.

ripple stimuli (Fig. 6), and are referred to as 'inconsistent non-linear' neurons.

The distributions of the f_1/f_0 ratios from our sample of 396 neurons are shown in Fig. 7. As the f_1/f_0 ratios were determined for each period histogram, we have plotted the data for each neuron as a mean ratio. This was calculated by averaging the ratios obtained from the range of period histograms at each ripple stimulus giving well-defined responses (Fig. 7*A*). In addition, we also show the distribution of these ratios obtained at the best modulated response of the neuron to the ripple stimulus (Fig. 7*B*). In both cases, these distributions are unimodal (dip test of unimodality; Hartigan & Hartigan, 1985) and peak around the ratio of 1.0 (Fig. 7*A*, mean ± s.d.,

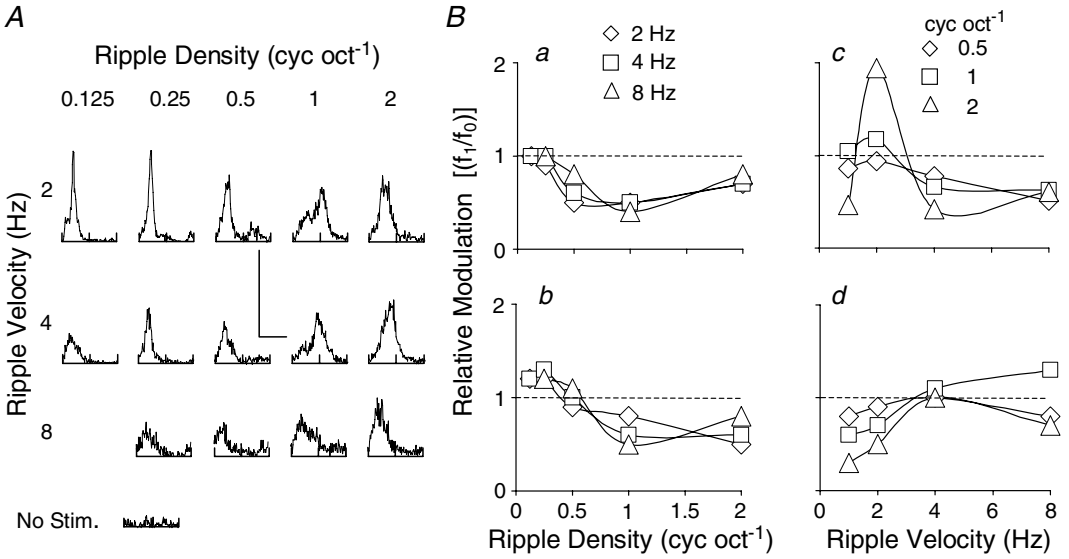

Figure 6. Inconsistent non-linear A1 neurons
The f_1/f_0 ratios from the period histograms in *A* are plotted in *Ba*. In *A*, the vertical calibration bar represents 120 spikes bin^{-1} at 2 and 4 Hz, and 60 spikes bin^{-1} at 8 Hz. Three further examples of these non-linear neurons are shown in *Bb–d*. Details as in Fig. 5.

1.09 ± 0.38; Fig. 7*B*, 1.08 ± 0.38). The distribution of f_1/f_0 ratios across samples of V1 neurons is commonly reported to be bimodal (Movshon *et al.* 1978*a*,*b*; Dean & Tolhurst, 1983; Mechler & Ringach, 2002). Our A1 results differ substantially from published V1 results, in that the distribution of f_1/f_0 ratios for our sample as a whole is clearly unimodal (Fig. 7*A* and *B*).

We also examined the distribution of f_1/f_0 ratios and linearity classes as a function of recording depth. Figure 8*A* shows the number of consistently linear and nonlinear units found at various depths. The numbers for locally linear and inconsistent non-linear units are shown in Fig. 8*B*. Overall, our data show a higher proportion of consistently linear and locally linear neurons at more superficial recording sites. To test whether the distribution of the different response classes varied as a function of depth, we constructed a contingency table, recording the number of neurons found in each category for a number of 200 μm wide depth bands (Table 1). A χ^2 test showed that the proportions of response classes were not independent of recording depth ($\chi^2 = 59.5$, d.f. $= 8$, $P < 10^{-9}$), indicating that the differences in the distribution of response classes as a function of depth are statistically significant.

Given the uneven distribution of response classes as a function of depth observed in Fig. 8*A* and *B* and Table 1, one would expect average f_1/f_0 ratios to vary also as a function of depth. This is indeed the case. The distribution of f_1/f_0 ratios for each of the recording depth bands are shown in Fig. 8*C*. Note that the median f_1/f_0 ratio is above 1.0 for recording depths less that 800 μm, and below 1.0 for depths greater than 800 μm. This trend as a function of depth was observed in both of the ferrets. It is of course possible, perhaps even to be expected, that response linearity may vary across the surface of A1 as much as it varies as a function of depth. To investigate this, we performed a two-way ANOVA test in which both recording depth (banded in 200 μm wide bands as in Table 1 and Fig. 8*C*) as well as horizontal position of the recording sites were considered as possible explanatory variables. Our data were collected from 11 separate penetrations with the multisite-array electrode, and each penetration as well as each depth band was considered as a separate 'factor' in this two-way ANOVA. The resulting ANOVA table is shown in Table 2. It is clear that there is a highly significant effect, both of penetration (i.e. horizontal position) as well

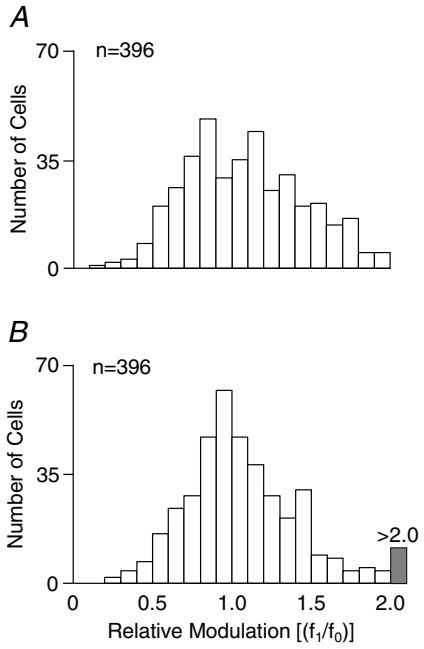

Figure 7. Distribution of f_1/f_0 ratios
A, distribution of f_1/f_0 ratios for the entire sample of 396 neurons, averaged over the range of ripple stimuli tested. *B*, f_1/f_0 ratios for the entire sample, calculated for the optimal ripple stimulus for each neuron.

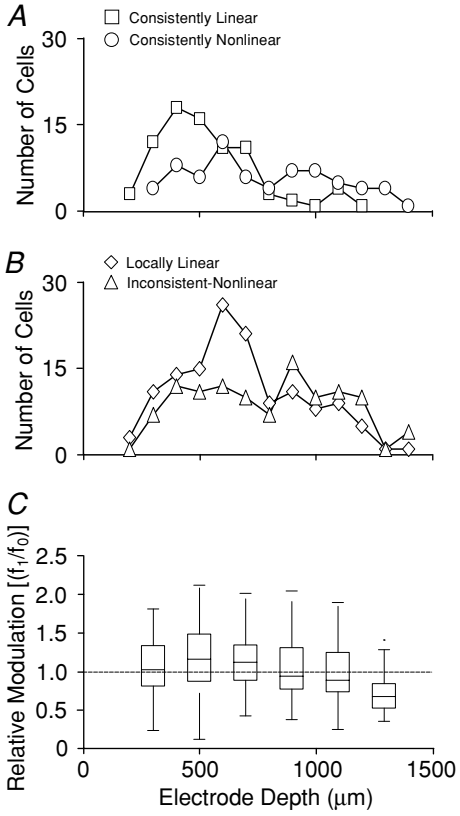

Figure 8. Distribution of response classes and mean f_1/f_0 ratios with recording depth
A, number of consistently linear (□) and consistently non-linear (○) neurons observed at each recording depth. *B*, number of locally linear (◇) and inconsistent non-linear (△) neurons observed at each recording depth. Both the consistently linear and locally linear (*B*, ◇) neurons predominate in the superficial cortex. *C*, 'box and whisker' plot showing the distribution of the mean f_1/f_0 ratios across all neurons as a function of depth. The boxes give the 25th, 50th (median) and 75th percentiles of the distribution at each depth. The whiskers extend out to the end of the observed range of values.

Table 1. 6 × 4 contingency table showing the number of units in each of the four response classes at each of six recording depths

Type\depth (μm)	200–400	400–600	600–800	800–1000	1000–1200	1200–1400
Consistently linear	15 (23%)	42 (37%)	17 (18%)	2 (4%)	6 (10%)	0 (0%)
Locally linear	21 (32%)	33 (29%)	43 (46%)	13 (28%)	21 (36%)	3 (15%)
Consistently non-linear	8 (12%)	15 (13%)	12 (13%)	8 (17%)	12 (21%)	7 (35%)
Inconsistent non-linear	22 (33%)	22 (20%)	21 (23%)	24 (51%)	19 (33%)	10 (50%)

The numbers in parentheses give the proportion of each class within each of the six depth bands.

Table 2. ANOVA table showing significance of variation in f_1/f_0 ratios as a function both of recording site and recording depth

Source	Sum of square	d.f.	Mean square	*F*	*P*
Penetration	9.29	10	0.929	7.92	$<10^{-10}$
Depth	5.17	5	1.034	0.81	$<10^{-8}$
Error	44.62	380	0.117		
Total	59.14	395			

as of depth. In terms of topographic location across the auditory cortex, no obvious order or systematic gradient was apparent in the arrangements of penetrations yielding, respectively, high or low average f_1/f_0 ratios (data not shown).

Discussion

We have examined the responses of primary auditory cortical neurons to a range of dynamic spectral ripple stimuli. Almost 75% of all recorded neurons gave modulated responses to the ripple stimuli, with 65% responding to a wide range of ripple velocities and densities. We found the magnitude of the responses varied with the ripple stimulus but, in general, neurons preferred low densities ($<$1.0 cycles oct^{-1}) and velocities ($<$8 Hz). The distribution of preferred ripple densities from our sample was in perfect agreement with that of Kowalski *et al.* (1996*a*). The only slight discrepancy from them was for ripple velocity where our sample peaked at a slightly lower velocity ($\sim$4 Hz instead of $\sim$8 Hz). Kowalski *et al.* (1996*a*) assumed response linearity, and constructed transfer functions for ripple velocity and ripple density, which allowed them to predict responses to arbitrary dynamic spectral ripple stimuli for 84% of their neurons (Kowalski *et al.* 1996*b*). In the present study, rather than assuming linearity, we have measured the f_1/f_0 ratio, a ratio that can be used as a quantitative estimate of response linearity. Based on this, 54.5% of our sample exhibited average f_1/f_0 ratios $>$1, a criterion value often used in studies of V1 to distinguish linear (simple) from non-linear (complex) cells.

The first studies that used the f_1/f_0 ratio as a measure of linearity in V1 were undertaken by Movshon *et al.* (1978*a*,*b*); they showed that the majority of simple cells had f_1/f_0 ratios greater than 1.0, and confirmed that these neurons spatially summated their responses to moving sine-wave gratings in an approximately linear manner. At constant contrast, the response linearity held for a range of spatial frequencies. For complex cells, however, the f_1/f_0 ratio was less than 1.0. This quantitative technique therefore was an adjunct to the original qualitative dichotomies put forward by Hubel & Wiesel (1962) into simple (spatial summation approximately linear) and complex (non-linear) cell categories (Movshon *et al.* 1978*a*,*b*; Dean & Tolhurst, 1983; Mechler & Ringach, 2002). Other studies have corroborated the correlation 'linearity' and 'simple cell' for visual cortex (De Valois *et al.* 1982; De Valois & Tootell, 1983; Bonds, 1989; Hamilton *et al.* 1989; Skottun *et al.* 1991; Ibbotson *et al.* 2005). The overall distribution of the relative modulation for V1 neurons, either from a single study (Dean & Tolhurst, 1983) or combined across many of these studies (Skottun *et al.* 1991), forms a bimodal distribution (a peak at $\sim$0.2 representing non-linear neurons, and a linear peak at $\sim$1.7) with a minimum around 1.0.

While only about 20% of our A1 neurons exhibited f_1/f_0 ratios consistently above 1.0, a further 34% of neurons were considered 'locally linear' because they maintained an f_1/f_0 ratio above 1.0 either over a range of ripple densities at a fixed ripple velocity or over a range of ripple velocities at a fixed ripple density. Movshon *et al.* (1978*a*) also found evidence of simple cells which were 'non-linear', and simple cells have been shown to have f_1/f_0 ratios below 1.0 for certain parameter ranges (Dean & Tolhurst, 1983). It may be tempting to suggest that our linear and locally linear neurons might be the A1 equivalent of V1 'simple' cells. However, the fact that neither the statistical nor the anatomical distribution of f_1/f_0 ratios found in A1 closely resembles that reported for V1 cautions against such an interpretation.

For our auditory cortex data, we have illustrated the distributions of the f_1/f_0 ratios based on mean values over a range of ripple stimuli (Fig. 7*A*) and on the value at a particular ripple velocity and density that gave the best response from the neuron (Fig. 7*B*). These distributions can be readily compared with those from the visual cortex. For example, Fig. 7*B* can be directly compared with Fig. 5 from Dean & Tolhurst (1983) and Fig. 2 from Skottun *et al.* (1991). Unlike the bimodal distributions from these

visual cortex data, we find distributions (Fig. 7*A* and *B*) with a single peak with the maxima at the f_1/f_0 relative modulation ratio close to 1.0. In auditory cortex therefore f_1/f_0 ratios reveal no 'natural boundary' between linear and non-linear classes. This difference between our ferret results from A1 and published V1 data is unlikely to be attributable to species differences, as simple cells are abundant in ferret visual cortex (Usrey *et al.* 2003), and a bimodal distribution has even been reported for the primary visual cortex in the marsupial Tammar wallaby (Ibbotson *et al.* 2005).

The evidence from our depth analysis is also intriguing. In ferret cortex, layer IV is typically found at a depth of approximately 700–900 μm. The predominance of consistently linear and locally linear neurons and average f_1/f_0 ratios at depths less than 700 μm would therefore indicate that the superficial layers (II–III) of A1 are processing information in a 'more linear' way, than the deeper layers (V–VI). Certainly, their outputs do project to distinct anatomical locations: superficial layer neurons project to a wide range of ipsilateral cortical areas, as well as to the contralateral primary auditory cortex (Wallace & Harper, 1997), whereas the deep layer neurons project to subcortical structures such as the ventral medial geniculate nucleus and the central nucleus of the inferior colliculus (Kelly & Wong, 1981). The primary visual cortex, in contrast, has abundant simple cells in layers IV and VI (Martinez *et al.* 2005) and it therefore seems that linear processing elements may not be distributed in the same way across the superficial and infragranular layers of A1 and V1, respectively.

We conclude that the primary auditory cortex has neurons that process incoming information both linearly and non-linearly. Unlike the visual cortex, auditory cortical neurons cannot easily be separated into two distinct classes based on their distribution of f_1/f_0 ratios. Linear-type neurons are found predominantly in the superficial layers, and integrate complex auditory stimuli, such as dynamic spectral ripple stimuli, over their best frequency by a straightforward summative approach, but it is doubtful whether they ought to be considered the auditory equivalent of V1 simple cells.

References

Aertsen AM & Johannesma PI (1981). A comparison of the spectro-temporal sensitivity of auditory neurons to tonal and natural stimuli. *Biol Cybern* **42**, 145–156.

Bonds AB (1989). Role of inhibition in the specification of orientation selectivity of cells in the cat striate cortex. *Vis Neurosci* **2**, 41–55.

De Valois RL, Albrecht DG & Thorell LG (1982). Spatial frequency selectivity of cells in macaque visual cortex. *Vision Res* **22**, 545–559.

De Valois KK & Tootell RBH (1983). Spatial frequency specific inhibition in cat striate cortex cells. *J Physiol* **336**, 359–376.

Dean AF & Tolhurst DJ (1983). On the distinctness of simple and complex cells in the visual cortex of the cat. *J Physiol* **344**, 305–325.

deCharms RC, Blake DT & Merzenich MM (1998). Optimizing sound features for cortical neurons. *Science* **280**, 1439–1443.

Hamilton DB, Albrecht DG & Geisler WS (1989). Visual cortical receptive fields in monkey and cat: spatial and temporal phase transfer function. *Vision Res* **29**, 1285–1308.

Hartigan JA & Hartigan PM (1985). The dip test of unimodality. *Ann Stat* **13**, 70–84.

Hubel DH & Wiesel TN (1959). Receptive fields of single neurones in the cat's striate cortex. *J Physiol* **148**, 574–591.

Hubel DH & Wiesel TN (1962). Receptive fields, binocular interaction and functional architecture in the cat's visual cortex. *J Physiol* **160**, 106–154.

Hubel DH & Wiesel TN (1968). Receptive fields and functional architecture of monkey striate cortex. *J Physiol* **195**, 215–243.

Ibbotson MR, Price NSC & Crowder NA (2005). On the division of cortical cells into simple and complex types: a comparative viewpoint. *J Neurophysiol* **93**, 3699–3702.

Joris PX, Schreiner CE & Rees A (2004). Neural processing of amplitude modulated sounds. *Physiol Rev* **84**, 541–577.

Kelly JP & Wong D (1981). Laminar connections of the cat's auditory cortex. *Brain Res* **212**, 1–15.

Kowalski N, Depireux DA & Shamma SA (1996*a*). Analysis of dynamic spectra in ferret primary auditory cortex. I. Characteristics of single-unit responses to moving ripple spectra. *J Neurophysiol* **76**, 3503–3523.

Kowalski N, Depireux DA & Shamma SA (1996*b*). Analysis of dynamic spectra in ferret primary auditory cortex. II. Prediction of unit responses to arbitrary dynamic spectra. *J Neurophysiol* **76**, 3524–3534.

Lu T, Liang L & Wang X (2001). Temporal and rate representations of time-varying signals in the auditory cortex of awake primates. *Nat Neurosci* **4**, 1131–1138.

Martinez LM, Wang Q, Reid RC, Pillai C, Alonso JM, Sommer FT & Hirsch JA (2005). Receptive field structure varies with layer in the primary visual cortex. *Nat Neurosci* **8**, 372–379.

Mechler F & Ringach DL (2002). On the classification of simple and complex cells. *Vision Res* **42**, 1017–1033.

Mendelson JR & Cynader MS (1985). Sensitivity of cat primary auditory cortex (A1) neurons to the direction and rate of frequency modulation. *Brain Res* **327**, 331–335.

Merzenich MM, Knight PL & Roth GL (1973). Cochleotopic organization of primary auditory cortex in the cat. *Brain Res* **63**, 343–346.

Merzenich MM, Knight PL & Roth GL (1975). Representation of cochlea within primary auditory cortex in the cat. *J Neurophysiol* **38**, 231–249.

Movshon JA, Thompson ID & Tolhurst DJ (1978*a*). Spatial summation in the receptive fields of simple cells in the cat's striate cortex. *J Physiol* **283**, 53–77.

Movshon JA, Thompson ID & Tolhurst DJ (1978*b*). Receptive field organization of complex cells in the cat's striate cortex. *J Physiol* **283**, 79–99.

Movshon JA, Thompson ID & Tolhurst DJ (1978*c*). Spatial and temporal contrast sensitivity of neurones in areas 17 and 18 of the cat's visual cortex. *J Physiol* **283**, 101–120.

Nelken I (2002). Feature detection by the auditory cortex. In *Integrative Functions in the Mammalian Auditory Pathway*, ed. Oertel D, Fay RR & Popper AN, pp. 358–416. Springer, New York.

Nelken I & Versnel H (2000). Responses to linear and logarithmic frequency-modulated sweeps in ferret primary auditory cortex. *Eur J Neurosci* **12**, 549–562.

Phillips DP & Irvine DRF (1981). Responses of single neurons in physiologically defined primary auditory cortex (A1) of the cat: frequency tuning and responses to intensity. *J Neurophysiol* **45**, 48–58.

Read HL, Jeffery AW & Schreiner CE (2002). Functional architecture of auditory cortex. *Curr Opin Neurobiol* **12**, 433–440.

Roe AW, Pallas SL, Kwon YH & Sur M (1992). Visual projections routed to the auditory pathway in ferrets: receptive fields of visual neurons in primary auditory cortex. *J Neurosci* **12**, 3651–3664.

Rutkowski RG, Shackleton TM, Schnupp JW, Wallace MN & Palmer AR (2002). Spectrotemporal receptive field properties of single units in the primary, dorsocaudal and ventrorostral auditory cortex of the guinea pig. *Audiol Neurootol* **7**, 214–227.

Schnupp JW, Mrsic-Flogel TD & King AJ (2001). Linear processing of spatial cues in primary auditory cortex. *Nature* **414**, 200–204.

Schreiner CE & Mendelson JR (1990). Functional topography of cat primary auditory cortex: distribution of integrated excitation. *J Neurophysiol* **64**, 1442–1459.

Schreiner CE & Urbas JV (1988). Representation of amplitude modulation in the auditory cortex of the cat. II. Comparison between cortical fields. *Hear Res* **32**, 49–64.

Sen K, Theunissen FE & Doupe AJ (2001). Feature analysis of natural sounds in the songbird auditory forebrain. *J Neurophysiol* **86**, 1445–1458.

Shamma SA & Versnel H (1995). Ripple analysis in ferret primary auditory cortex. II. Prediction of unit responses to arbitrary spectral profiles. *Aud Neurosci* **1**, 255–270.

Shamma SA, Versnel H & Kowalski N (1995). Ripple analysis in ferret primary auditory cortex. I. Response characteristics of single units to sinusoidally rippled spectra. *Aud Neurosci* **1**, 233–254.

Skottun BC, De Valois RL, Grosof DH, Movshon JA, Albrecht DG & Bonds AB (1991). Classifying simple and complex cells on the basis of response modulation. *Vision Res* **31**, 1079–1086.

Theunissen FE, Sen K & Doupe AJ (2000). Spectral-temporal receptive fields of nonlinear auditory neurons obtained using natural sounds. *J Neurosci* **20**, 2315–2331.

Usrey WM, Sceniak MP & Chapman B (2003). Receptive fields and response properties of neurons in layer 4 of ferret visual cortex. *J Neurophysiol* **89**, 1003–1015.

Versnel H, Kowalski N & Shamma SA (1995). Ripple analysis in ferret primary auditory cortex. III. Topographic distribution of ripple response parameters. *Aud Neurosci* **1**, 271–285.

Wallace MN & Harper MS (1997). Callosal connections of the ferret primary auditory cortex. *Exp Brain Res* **116**, 367–374.

Acknowledgements

This work was supported by BBSRC (UK) grant 43/S19595, and NIH/NCRR grant P41 RR09754.